

# Cost- and time-effective three-dimensional bone-shape reconstruction from X-ray images

Murat Gunay  
Mun-Bo Shim  
Kenji Shimada\*

*Department of Mechanical Engineering, Carnegie Mellon University, Pittsburgh, PA 15213, USA*

\*Correspondence to: Kenji Shimada, Department of Mechanical Engineering, Carnegie Mellon University, 5000 Forbes Avenue, Pittsburgh, PA 15213, USA. E-mail: shimada@cmu.edu

## Abstract

**Background** Three-dimensional (3D) bone shapes need to be created for visualization and pre-operative surgery planning. Conventionally such shape data is extracted from volumetric data sets, obtained by three-dimensional sensors, such as computerized tomography (CT) and magnetic resonance imaging (MRI). This conventional method is highly labor intensive and time consuming.

**Methods** This paper presents a cost- and time-effective computational method for generating a 3D bone shape from multiple X-ray images. Starting with a predefined 3D template bone shape that is clinically normal and scaled to an average size, our method scales and deforms the template shape until the deformed shape gives an image similar to an input X-ray image when projected onto a two-dimensional (2D) plane. The hierarchical freeform deformation method is used to scale and deform the template bone. The problem of finding the 3D shape of the bone is reduced to a sequence of optimization problems. The objective of this optimization is to minimize the error between the input X-ray image and the projected image of the deformed template shape. The sequential quadratic programming (SQP) is used to solve this multi-dimensional optimization problem.

**Results** The proposed X-ray image-based shape reconstruction is more computationally efficient, cost-effective and portable compared to the conventional CT- or MRI-based methods. Within a couple of minutes with a standard personal computer, the proposed method generates a 3D bone shape that is sufficiently accurate for many applications, such as (a) making a 3D physical mock-up for training and (b) importing into, and using in, a computer-aided planning system for orthopedic surgery, including bone distraction and open/closed wedge osteotomy.

**Conclusions** Because the proposed method requires only a small number of X-ray images and a minimum input from the user, the method can serve as a cost- and time-effective 3D bone shape reconstruction method for various medical applications. Copyright © 2008 John Wiley & Sons, Ltd.

**Keywords** geometrical reconstruction; free-form deformation; computer-assisted surgery; three-dimensional modelling

## Introduction

This paper presents a cost- and time-effective computational method for generating a three-dimensional (3D) bone geometry from a few X-ray images. The resulting 3D shape is adequately accurate and useful in most

Accepted: 30 October 2007

situations where: (a) 3D geometry is needed for computer-aided planning of orthopaedic surgeries, including bone distraction and open/closed wedge osteotomy; or (b) a 3D physical mock-up is required for training and education.

3D bone geometries are necessary for visualization and pre-operative surgery planning. They are typically extracted from volumetric datasets obtained by 3D sensors, such as computed tomography (CT) and magnetic resonance imaging (MRI). The surface of a bone can be extracted from the volumetric data by using the marching cube algorithm (1). Although CT-based methods provide straightforward and versatile solutions for general 3D geometry reconstruction problems, the boundary edge extraction in their systems is not fully automatic and is a time-consuming process.

Our goal is to provide another simple, portable, cost- and time-effective option for creating a 3D bone geometry using X-ray images. The new computational method proposed here is based on the hierarchical free-form deformation and numerical optimization of deformation parameters. Starting with a predefined 3D template bone shape, clinically normal and scaled to average size, our method scales and deforms the template shape until the deformed shape produces an image similar to an input X-ray image when projected onto a two-dimensional (2D) plane. The control lattice of free-form deformation is hierarchically subdivided in the area where 2D error is higher than the given threshold. Finding the 3D shape of the bone is, thus, reduced to an optimization problem that minimizes the 2D error, or the difference between the input X-ray image and the projected image of the deformed template bone shape. We use sequential quadratic programming (SQP) (4) to solve the multi-dimensional non-linear optimization problem.

Through the experimental results, it is shown that the proposed X-ray-based 3D bone geometry reconstruction is sufficiently accurate for pre-operative planning, intra-operative registration and post-operative evaluation of the majority of osteotomy and distraction cases.

The rest of this paper is organized as follows. After reviewing previous work, we give a formal statement of our shape reconstruction problem; the proposed technical approach is then outlined; next, the results of computational experiments using the proposed method are presented, along with some discussion; and finally, we make some concluding remarks and suggest future work.

## Previous work on 3D shape reconstruction

There are two categories of methods to create a 3D shape of an object; one is to extract boundaries of object surfaces from a volumetric dataset obtained by CT or MRI, and the other is to reconstruct a 3D shape from single or multiple 2D drawing(s) or image(s). In this section, we do not review methods in the first category because there is a

comprehensive literature survey available (5). Instead, in the rest of this section, we review previous methods for reconstructing a 3D shape from single or multiple 2D drawings and images.

The problem of 3D shape reconstruction from 2D data has been studied in at least two areas of research: (a) computer vision and (b) geometric modelling. Previous work in each area has a different problem statement and set of requirements and assumption. None of the proposed solutions addresses our 3D bone shape reconstruction problem perfectly.

For example, most computer-vision algorithms are designed so that they can handle general objects; they do not take advantage of the fact that the topology and rough geometry of a bone is known, and thus they are not efficient. Some work in computer vision uses pattern recognition techniques based on heuristics. A set of 2D elementary graphical elements (i.e. straight lines, rectangles, arcs and circles) is defined to represent projections. A classification process is then applied to these elements in order to cluster them according to distinct pattern characteristics. The heuristic search is then applied to find the possible patterns that match objects shown in the image. The algorithms are applicable only to objects of uniform thickness and the solutions they generate cannot recover the entire 3D semantics of an object (6).

The geometric modelling research community has also worked on the reconstruction of a 3D model from orthographic engineering drawings, in which an object is represented by 2D geometric primitives, such as points, lines and arcs (2,3,5,7–10). A typical reconstruction algorithm consists of the following steps (10): (a) generate candidate 3D vertices from 2D nodes; (b) construct 3D edges from 3D vertices; (c) form face loops of the object from 3D edges; (d) build components of the object from face loops; and (e) combine components to find the final solution.

Although 3D shape reconstruction from engineering drawings has been studied intensively and there are some commercial systems available, shapes reconstructed by these systems are limited to a certain class of geometry – solids bounded by a set of planes, quadric surfaces and tori. These previous methods in geometric modelling are thus not applicable to solving our shape reconstruction problem for free-formed bones. A more comprehensive literature review on 3D shape reconstruction can be found in (6).

## Problem statement

The 3D bone shape reconstruction problem that we are interested in can be stated as follows:

*Given:* X-ray images of a bone taken from different directions, and a template 3D bone shape that is clinically normal and scaled to the average size.

*Generate:* a 3D bone shape that matches the input X-ray images.

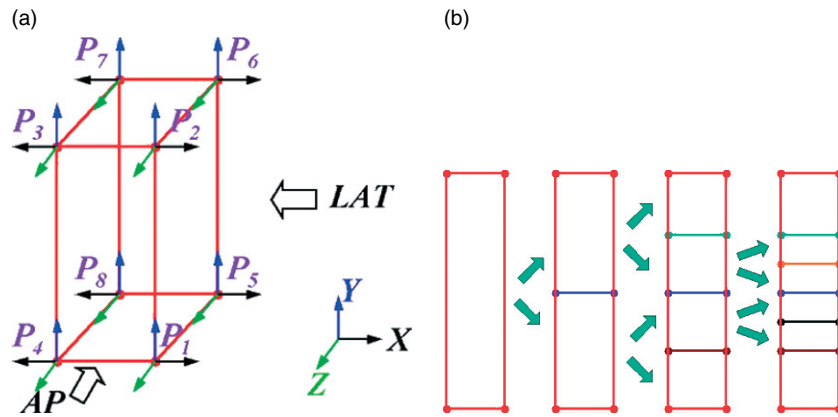


Figure 1. Hierarchical free-form deformation lattice: (a) deformation parameters; (b) binary tree subdivision

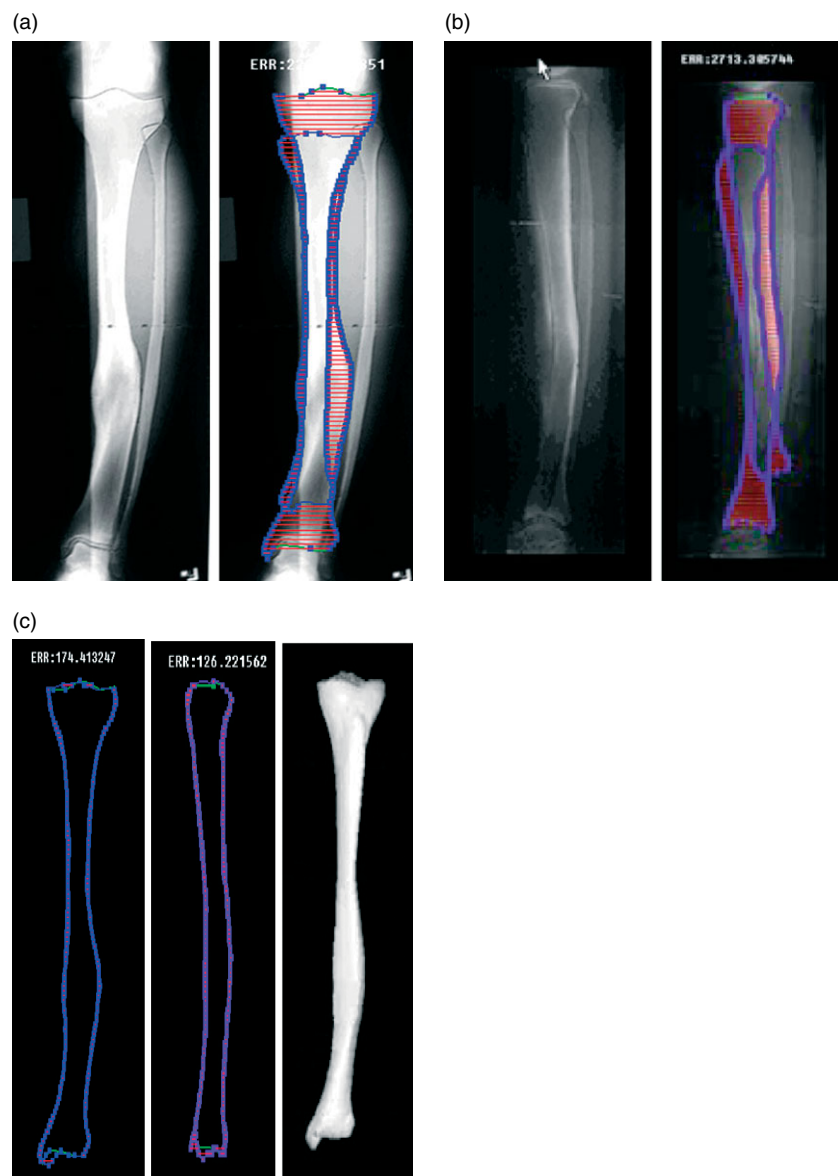


Figure 2. Input X-ray images and output 3D tibia shape generated: (a) input anteroposterior (AP) view; (b) input lateral (LAT) view; (c) matched silhouette boundaries and the output 3D shape

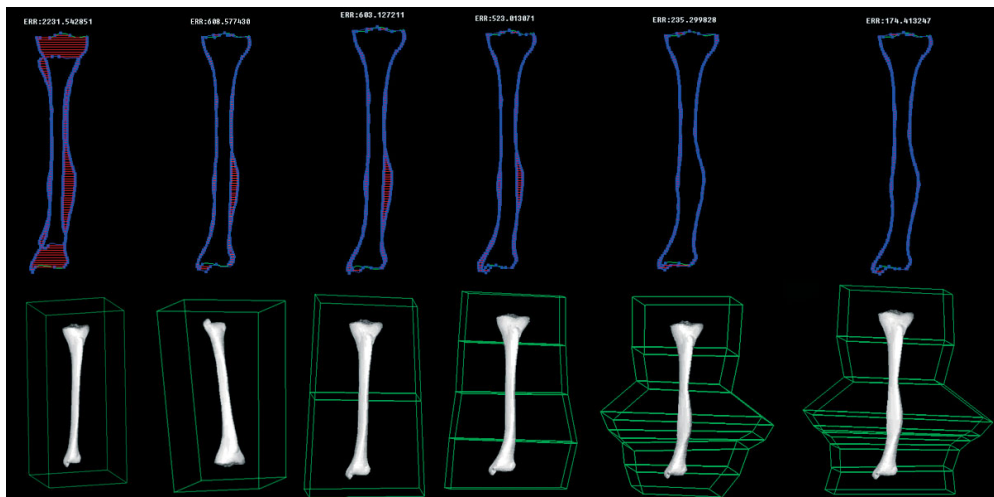


Figure 3. Hierarchical free-form deformation process

The X-ray images can be taken from any direction, but are usually front (anteroposterior, or AP) and side (lateral, or LAT). The camera calibration algorithm computes the camera model for each X-ray image by using a small X-ray marker (6). The control lattice is created so that it is perpendicular to the principal ray of the camera model. The template bone shape is then embedded inside the control lattice and deformed to match the X-ray image. This process is applied repeatedly through all the X-ray images to reconstruct the 3D bone shape. The details of this process are discussed below.

The template 3D bone shape is represented as a closed shell of a polygonal mesh, consisting of a set of vertices and a set of faces. It is important that there be no gap

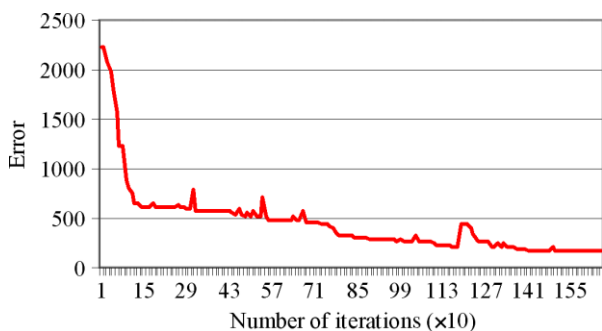


Figure 4. Minimized error between silhouette boundaries of X-ray images and template bone shape

or overlap between faces. Any gap or overlap will make it impossible to create a physical mock-up by using a rapid prototyping process. Also, the resolution of the template bone shape should be sufficiently fine so that small features of its shape will still be visible after the template bone geometry is deformed. One alternative to the polygonal mesh model of a template bone shape is to use a model consisting of parametric surfaces, such as Bézier surfaces and non-uniform rational B-spline surfaces (NURBS). Although a parametric surface-based model would increase the accuracy, our current template polygonal model with 1906 vertices and 3808 triangular polygons, which we purchased from a commercial vender, has sufficient resolution for most orthopaedic applications. If more resolution in the template bone geometry is necessary, available higher-resolution template bone geometry can be used. This higher-resolution bone geometry is generated by CT-scanning a healthy bone with a small slice thickness.

The proposed method generates a 3D bone shape represented as a polygonal mesh model. This output 3D bone shape can be used to make a 3D physical mock-up of the bone, or it can be used in a computer-assisted orthopaedic surgery planning system. Since we compute the camera model for each X-ray image by using a X-ray marker, the system can take more than two X-ray images taken from non-orthogonal directions (6).

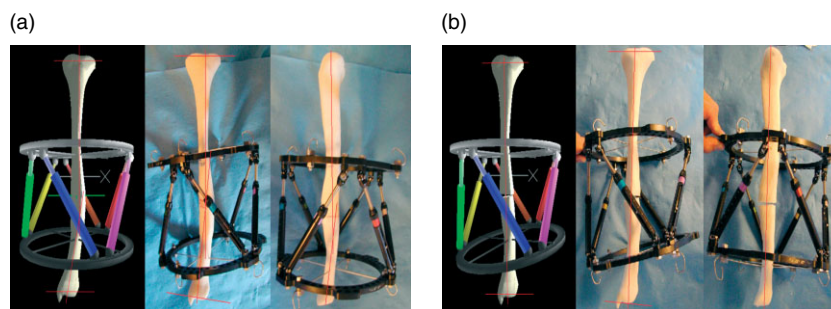


Figure 5. Mock surgery of correction with rapid prototype model: (a) before distraction; (b) after distraction

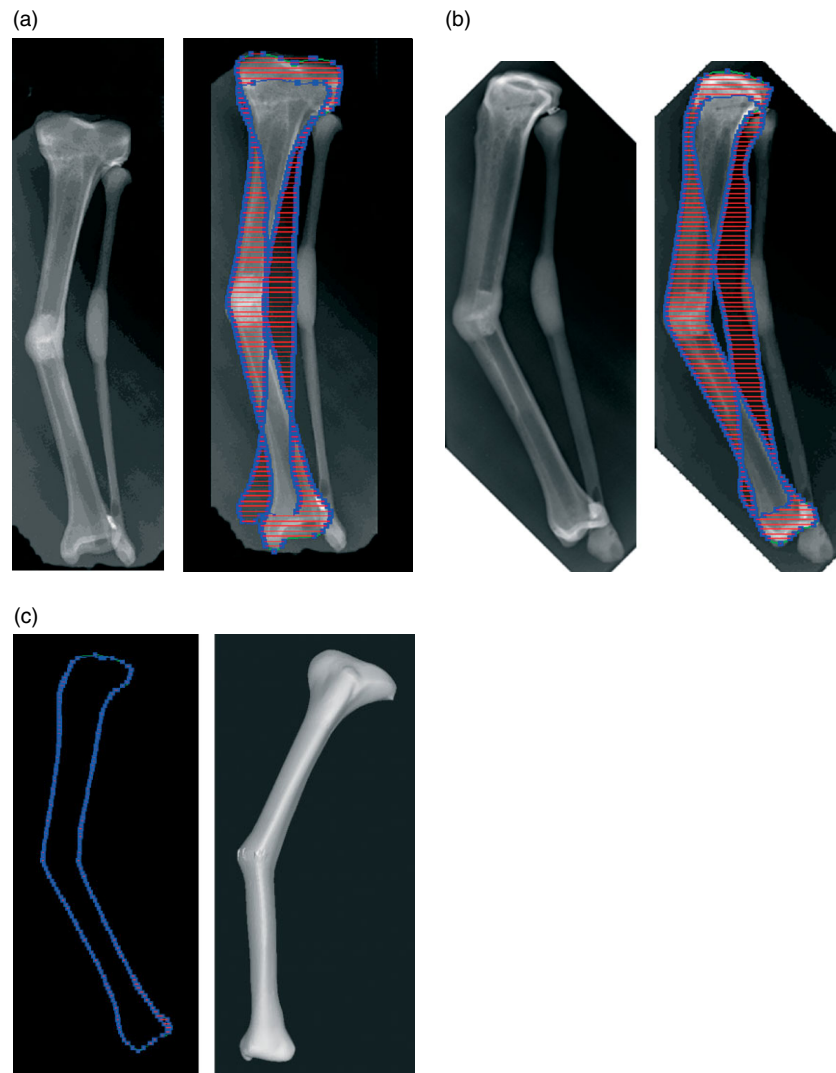


Figure 6. Input X-ray images and reconstructed 3D tibia shape: (a) input AP view; (b) input LAT view; (c) matched silhouette boundaries and the output 3D shape

## Technical approach

In this section we propose a technical approach to solving our bone shape reconstruction problem using: (a) hierarchical free-form deformation; and (b) deformation-parameter optimization.

We consider the following in designing the actual computational methods. For an efficient and robust shape reconstruction, we should utilize our knowledge of: (a) the type of bone shown in the given X-ray images; (b) the shape and size of a standard, or clinically normal, bone; and (c) the typical deformation modes and amount of deformation. This justifies our use of a template-based deformation approach, detailed in the following subsection. Also, because each patient's bone is different in size, deformation mode and the amount of deformation, we should construct our computational methods so that they work in a hierarchical manner, i.e. starting from a global deformation and gradually adding local deformations. We thus define the deformation lattice

hierarchically and solve the optimization of deformation parameters hierarchically.

### Hierarchical free-form deformation

Deformation of a 3D polygonal mesh has been studied intensively in the computer graphics research community for geometric design and animation. In this paper we deform a 3D template bone shape using a method based on one such deformation technique, Sederberg's free-form deformation (FFD) (11).

There are two new aspects in using this well-known FFD technique in our work: (a) FFD is applied to a new area of application, 3D shape reconstruction from 2D images, instead of to the traditional application domains of geometric modelling and animation; and (b) hierarchical and recursive refinement is applied to the control lattice of FFD to adjust the deformation resolution. We need to utilize hierarchical refinement because of the unique nature of our shape reconstruction problem; i.e.

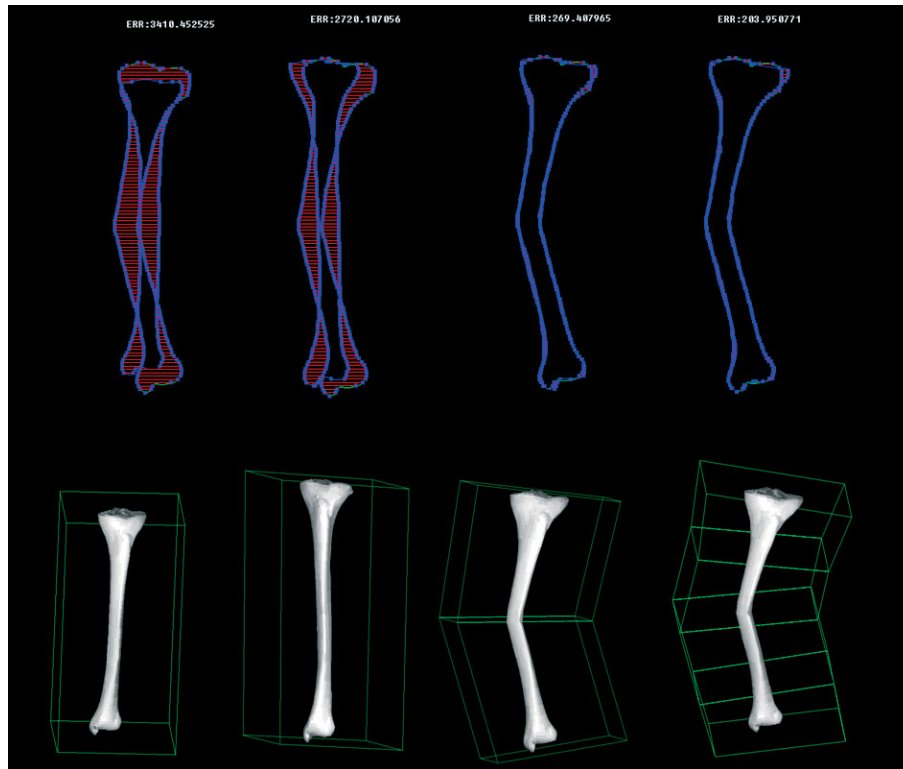


Figure 7. Hierarchical free-form deformation process of tibial osteotomy case

we do not know *a priori* the complexity or severity of the deformation.

The basic idea of Sederberg's FFD is that, instead of deforming the object directly, the object is embedded in a rectangular space that is deformable. One physical and intuitive analogy of FFD is that a flexible object is 'moulded' in a clear plastic block and the whole block is deformed by stretching, twisting, squeezing and so on. As the plastic block is deformed, the object trapped inside the block is also deformed accordingly. Sederberg uses the following single Bézier hyperpatch to perform this deformation:

$$\mathbf{q}(u, v, w) = \sum_{i=0}^n \sum_{j=0}^n \sum_{k=0}^n \mathbf{p}_{ijk} B_i(u) B_j(v) B_k(w) \quad (1)$$

$$0 \leq u \leq 1, 0 \leq v \leq 1, 0 \leq w \leq 1$$

where  $u$ ,  $v$ , and  $w$  are parameter values that specify the location of an original point in the control block space,  $\mathbf{q}(u, v, w)$  is the location of the point after the deformation,  $\mathbf{p}_{ijk}$  are points that define a control lattice, and  $B_i(u)$ ,  $B_j(v)$ , and  $B_k(w)$  are the Bernstein polynomials of degree  $n$ , for example:

$$B_i(u) = \frac{n!}{i!(n-i)!} u^i (1-u)^{n-i} \quad (2)$$

There are two approaches to deforming the template shape: (a) use a higher-order deformation function with one control lattice; or (b) use a linear deformation function with many control lattices and control points. The optimization problem with many control points, or

optimization parameters, is difficult to solve; however, the control lattice is subdivided hierarchically, which subdivides the control lattice in the place in which the error is greater than the predefined limit value, with fewer control points. This approach avoids subdividing the control lattice in unnecessary locations and thus reduces the computational cost significantly. In our system we use a linear version of FFD as a unit deformable block. This is the simplest deformation function, and there are only eight control points,  $\mathbf{p}_i$ ,  $i = 1, 2, \dots, 8$ , as shown in Figure 1a, and they define eight corner points of a deformable block. Since each point has three translational degrees of freedom,  $x_i$ ,  $y_i$  and  $z_i$ , and each control block has eight control points, there are  $8 \times 3 = 24$  degrees of freedom in total. The variation of a deformation with a linear function is limited compared to a higher-order function, but we choose to use the linear function because the complexity of the deformation of a bone is unknown, usually local, and we would rather increase the resolution of a deformation as needed by using adaptive refinement of the control lattice.

We perform this adaptive refinement by using a hierarchical, recursive, binary-tree subdivision of the control lattice, as shown in Figure 1b. We prefer the binary-tree subdivision, rather than a more standard spatial subdivision of octree subdivision, because our current target bones are mainly rims, which are cylindrically shaped. Octree would be a better choice when a target bone shape is not cylindrical. The extension from binary subdivision to octree subdivision is straightforward.

### Optimization of deformation parameters

Now that we have a way to freely deform a 3D template bone shape, as described in the previous section, the problem of finding the 3D shape of the bone is reduced to an optimization problem, in which the optimum combination of deformation parameters is searched and the objective is to minimize the error, or difference between the input X-ray images and the projected images of the deformed template shape.

There are two important technical issues to be addressed in order to solve our shape reconstruction problem both robustly and efficiently: how should we measure the error between the input AP and LAT X-ray images and the deformed 3D template bone?; and shall we perform the parameter optimization using the X-ray images at once or separately in sequence?

Regarding the first question, in the current implementation we choose to utilize silhouette boundaries. We define a closed silhouette boundary of the bone in each of the X-ray images. A corresponding closed-silhouette boundary of the deformed template 3D bone is also computed by projection of the 3D shape to a 2D plane. Because our goal is to deform the template bone shape until its silhouette boundary approaches as closely as possible that of the X-ray images, it becomes a simple task to measure the area difference between the two silhouette boundaries and utilize this quantity as the objective function to be minimized. We denote this area difference  $A$ , and it is a function of all the deformation parameters, i.e.:

$$A(x_1, \dots, x_8, y_1, \dots, y_8, z_1, \dots, z_8) \tag{3}$$

Alternatively, we could define an error function based on a set of fiducial points, the image intensity, or a combination of these with the above-mentioned silhouette boundary, but our initial experiments show that the silhouette boundary can be easily identified in an X-ray image, and the computation of a boundary silhouette from the shape of a deformed template bone is efficient.

The second technical issue, whether we should perform the parameter optimization using the X-ray images at once or separately in sequence, is also critical in making the optimization process more robust and efficient. With the camera modelling presented in (6), we should proceed

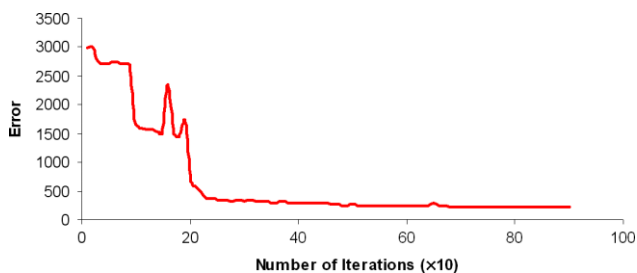


Figure 8. Minimized error between silhouette boundaries of X-ray images and template bone shape of tibial osteotomy case study

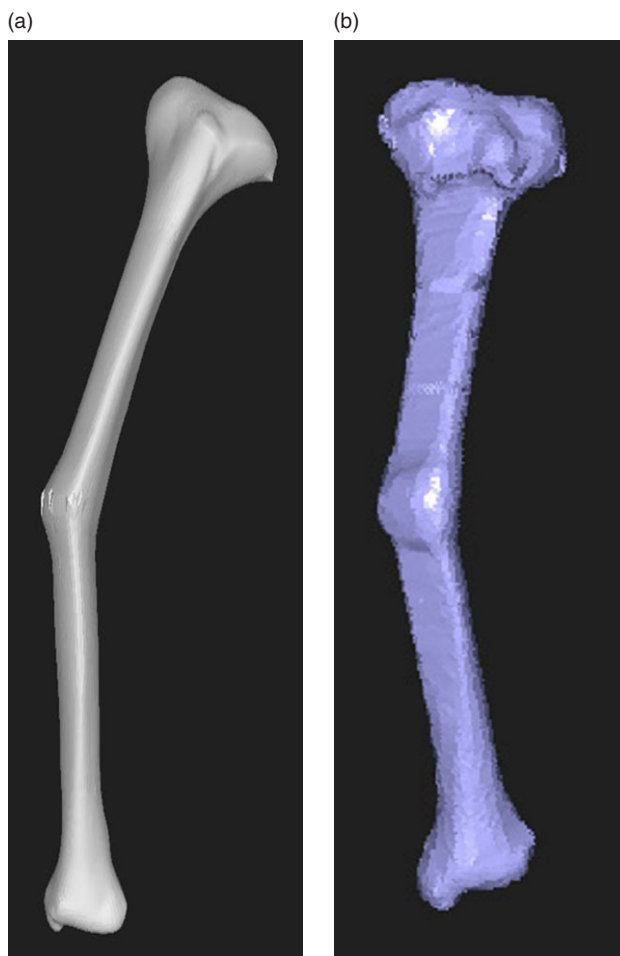


Figure 9. Osteotomy angle comparison: (a) reconstructed (40°); (b) CT-scanned (38°)

with the optimization for each image separately. In deforming the template bone using the AP view, we can assume there is no displacement in the  $z$  direction, i.e.  $z_i = 0, i = 1, \dots, 8$ , and the four pairs of points,  $(p_1, p_5), (p_2, p_6), (p_3, p_7), (p_4, p_8)$ , move together, i.e.  $x_1 = x_5, x_2 = x_6, x_3 = x_7, x_4 = x_8, y_1 = y_5, y_2 = y_6, y_3 = y_7, \text{ and } y_4 = y_8$ . These conditions together reduce the number of optimization parameters from 24 to eight. Since a multidimensional optimization problem like ours becomes much more unstable and time-consuming as the number of parameters to be optimized increases, reducing the number of parameters by two-thirds improves the robustness and the computational cost drastically. The optimization problem for the one FFD block for the AP view is thus stated as:

$$\begin{aligned} &\text{minimize : } A(x_1, x_2, x_3, x_4, y_1, y_2, y_3, y_4) \\ &\text{subject to : } -\Delta_x < x_i < \Delta_x, -\Delta_y < y_i < \Delta_y, i = 1, \dots, 4 \end{aligned}$$

where  $\Delta_x$  is the maximum displacement of a control point in the  $x$  direction and  $\Delta_y$  in the  $y$  direction. The optimization problem for one control lattice using other views can be formulated similarly. To solve the above optimization problem with eight deformation parameters,

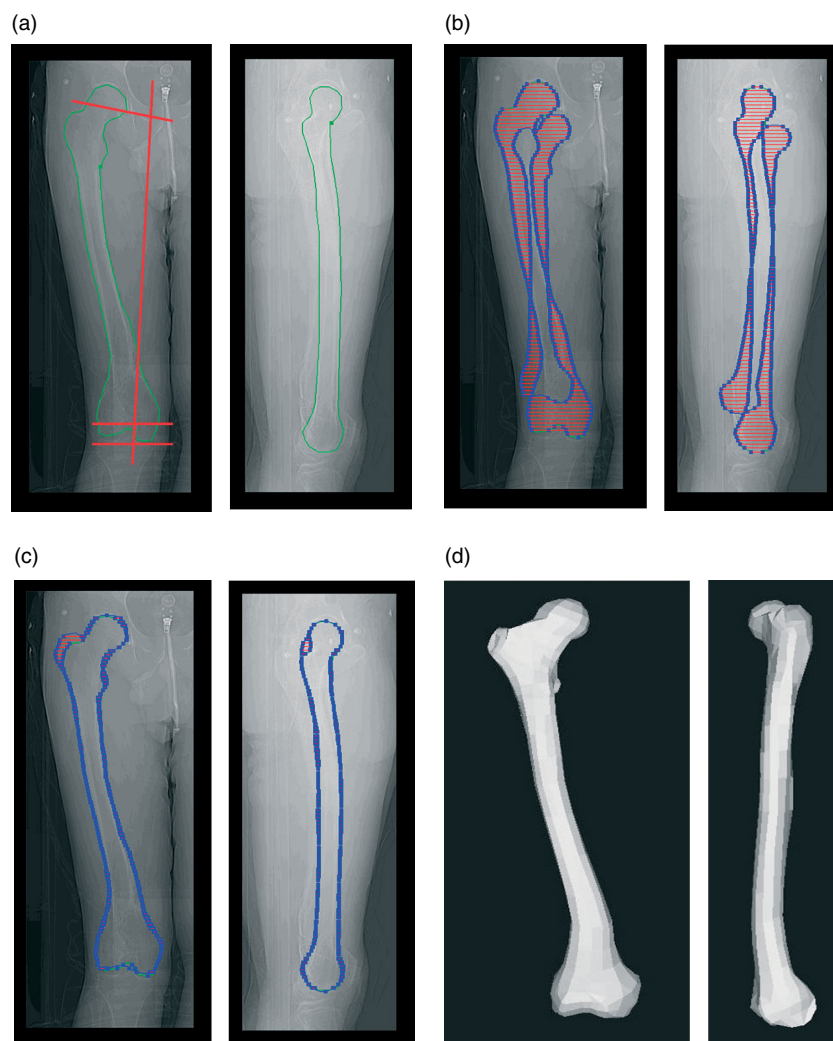


Figure 10. Femoral osteotomy: (a) AP and LAT X-rays; (b) initial error on AP and LAT images; (c) final error on AP and LAT images; (d) reconstructed bone geometry

we use the sequential quadratic programming (SQP) algorithm (4,6).

## Results

This section presents results obtained by the reconstruction method proposed in this paper. The reduction of 2D error during the reconstruction process was confirmed for all the test cases. The final output, a 3D bone shape, is presented for each of these case studies. Since the proposed reconstruction method hierarchically subdivides the control lattice of free-form deformation, we demonstrate that the reconstruction algorithm matches given X-ray images with the projection of the deformed template bone shape much better every time the hierarchical subdivision occurs. The system is implemented in C++ and runs on a PC with a Windows® operating system. The computational time required for generating a final tibia shape is less than 100s on an AMD 1.0 GHz PC. The computational time for the other cases is also within 2 min.

## Case study: bone distraction

The purpose of this case study is to demonstrate that the proposed reconstruction method can accommodate a locally deformed bone, typical in bone distraction surgery. The patient's X-ray images are taken in the AP and LAT directions, as shown in Figure 2a, b, to be used in the proposed reconstruction method. Figure 2c shows the output 3D geometry of the tibia. Figure 3 shows the process of hierarchical free-form deformation using the AP view. The first row of the figure depicts the convergence process of the two silhouette boundaries, one from the X-ray image and the other from the deformed template bone. Note that the bottom of the tibia is more severely deformed and that the finer deformation lattices are used in this region. Figure 4 shows how the errors between the silhouette boundary of X-ray images and the template bone shape are minimized through the optimization process.

The results of the bone distraction depicted in Figure 5 demonstrate the pre-operative surgery planner for bone distraction. The surgery planning results of this bone

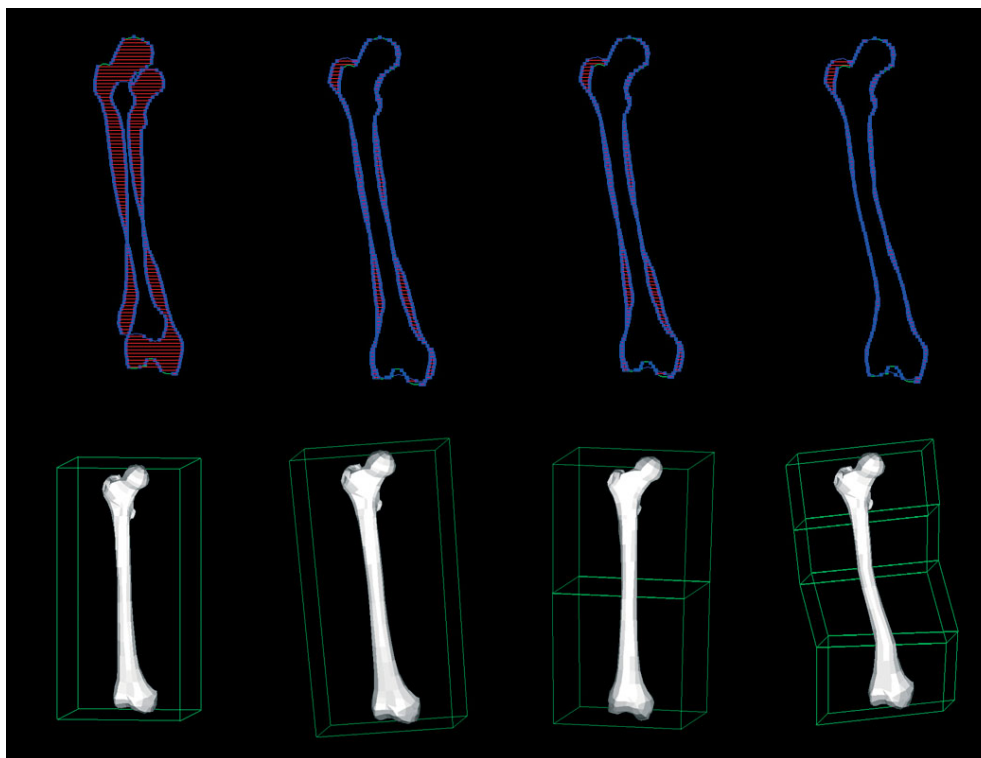


Figure 11. Hierarchical free-form deformation process of femoral osteotomy case

distraction are applied to the simulated surgery shown in the same figure. The surgery planner’s results match the outcomes of the simulated surgery. The reconstructed 3D bone shape is thus sufficiently accurate for bone distraction surgery.

**Case study: tibial osteotomy**

The purpose of this case study is to demonstrate that the proposed reconstruction method can create a bone geometry with a sufficiently accurate bent angle for an osteotomy surgery. Hence, the X-ray images of the tibia are taken from the AP and LAT directions, as shown in Figure 6, to be used in the proposed reconstruction method. Figure 7 shows the hierarchical deformation

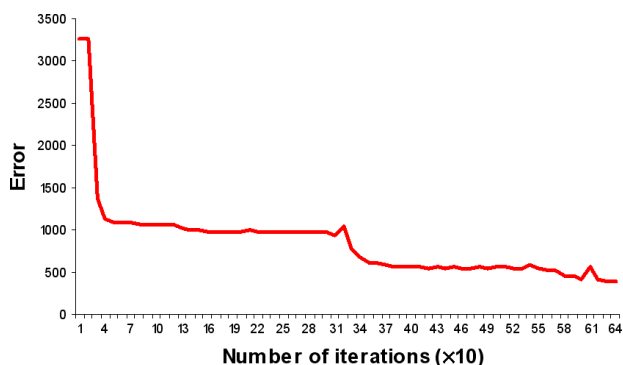


Figure 12. Minimized error between silhouette boundaries of X-ray images and template bone shape of femoral osteotomy case study

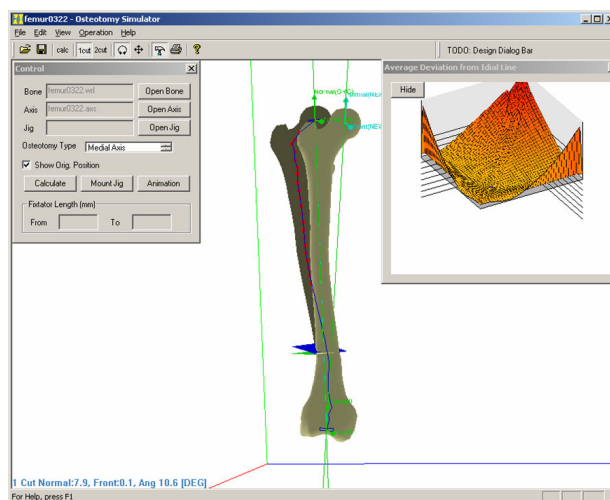


Figure 13. Optimal cutting location and angle of osteotomy

process using the AP view for the osteotomy study. The first row of the figure depicts the convergence process of the two silhouette boundaries: one from the X-ray image and the other from the deformed template bone. Figure 8 shows how the error between the silhouette boundaries of X-ray images and template bone shape is minimized through the optimization process. The figure also shows how the optimization process converges.

The tibia model of the osteotomy case is scanned with a CT scanner to validate the accuracy of the proposed method. Since accurate estimation of the deformation angle is crucial in osteotomy, the deformation angles for

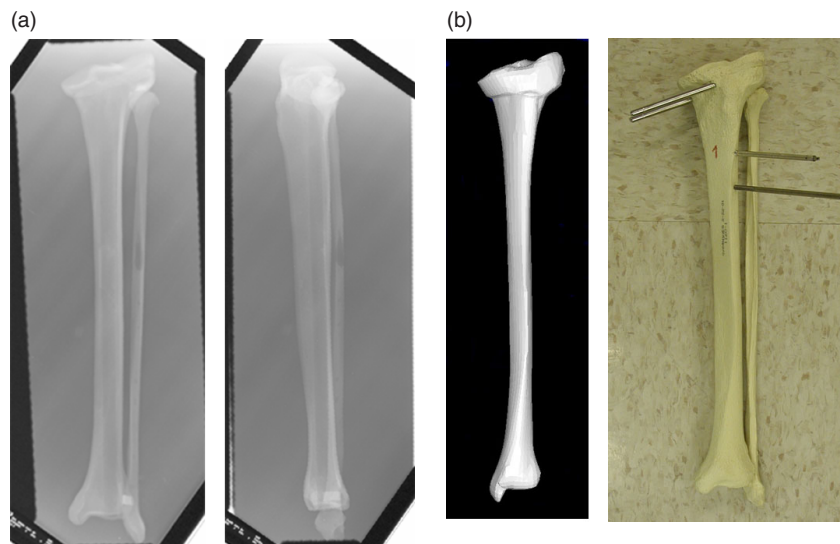


Figure 14. High tibial osteotomy: (a) AP and LAT X-ray images; (b) reconstructed shape and tibia

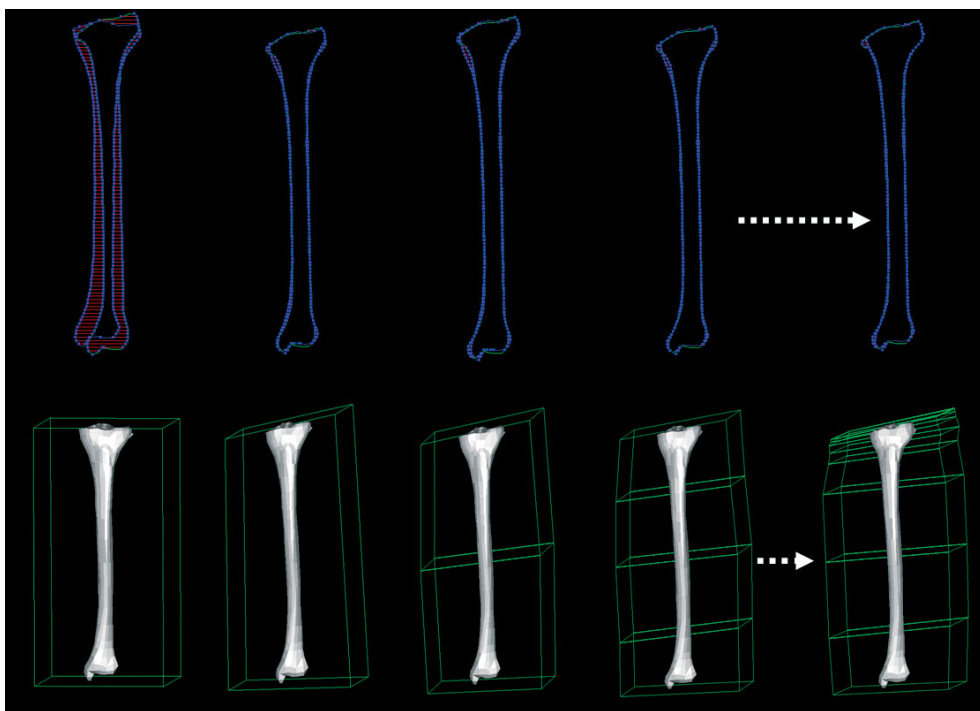


Figure 15. Hierarchical free-form deformation process of femoral osteotomy case

the models are measured by fitting circular cross-sections. The deformation angle of the output model from the proposed reconstruction method is only 2° different from the CT-based method, as shown in Figure 9. The accuracy of the proposed reconstruction method is sufficiently close to that of the CT-based reconstruction method for pre-operative planning of osteotomy. Figure 8 shows the converging process of the 2D error between the bone contour of the X-ray image and the silhouette boundaries of the template bone model. The spikes in the graph correspond to the hierarchical subdivision of the control lattice. The spikes occur because the optimization parameters are re-initialized after each hierarchical subdivision.

**Case study: femoral osteotomy**

The purpose of this case study was to demonstrate that the proposed reconstruction method can create a bone geometry with a sufficiently accurate osteotomy angle for a femoral osteotomy surgery. X-ray images of the patient’s right femur are taken from the AP and LAT directions, as shown in Figure 10, to be used in the proposed reconstruction method. Figure 11 shows the hierarchical deformation process using the AP view in the femoral osteotomy case. The first row of the figure depicts the convergence process of the two silhouette boundaries: one from the X-ray image, and the other from the deformed template

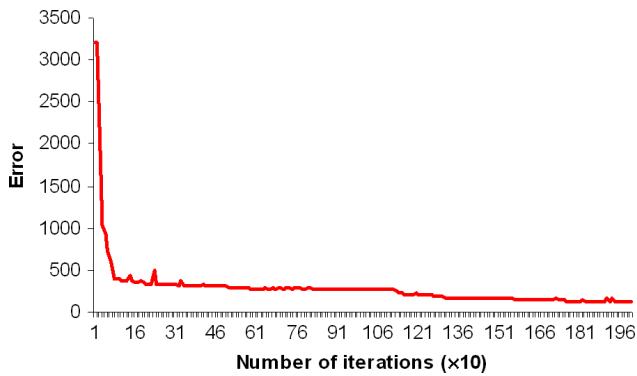


Figure 16. Minimized error between silhouette boundaries of X-ray images and template bone shape of HTO case study

bone. Figure 11 shows how the error between the silhouette boundaries of X-ray images and template bone shape is minimized through the optimization process. Based on these AP and LAT X-ray images of the patient, the 3D femur shape is generated by using the proposed reconstruction method, as shown in Figure 10. Figure 12 shows how quickly the optimization process converges.

Our osteotomy planner software, shown in Figure 13, computes the optimal location for cutting and the osteotomy angle for correction. This planner computed  $10.6^\circ$  as the necessary angular correction for this femoral osteotomy, and the orthopaedic surgeon who executed this surgery reported approximately  $11^\circ$  of correction by the conventional planning method based on 2D hand drawings. The femoral osteotomy study results thus show that the proposed reconstruction method creates sufficiently accurate 3D bone shape for femoral osteotomy.

### Case study: high tibial osteotomy (HTO)

The purpose of this case study is to demonstrate that the proposed reconstruction method can create a bone geometry with a sufficiently accurate osteotomy angle for high tibial osteotomy surgery. Therefore, the X-ray images of a tibia with high deformity are taken from the AP and LAT directions, as shown in Figure 14. These AP and LAT X-ray images are then used in the presented reconstruction algorithm to generate a 3D shape of the tibia, as depicted

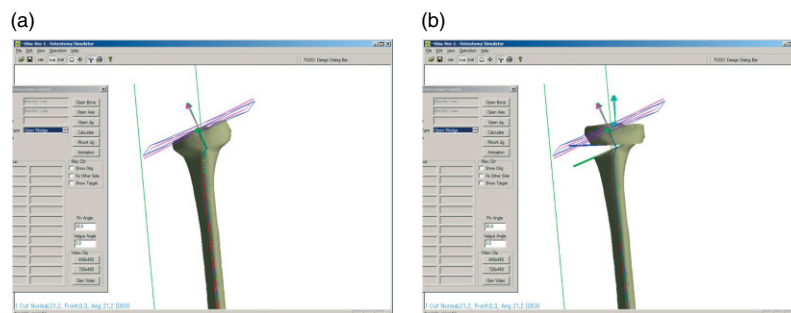


Figure 17. Surgical planner for high tibial osteotomy: (a) initial; (b) target

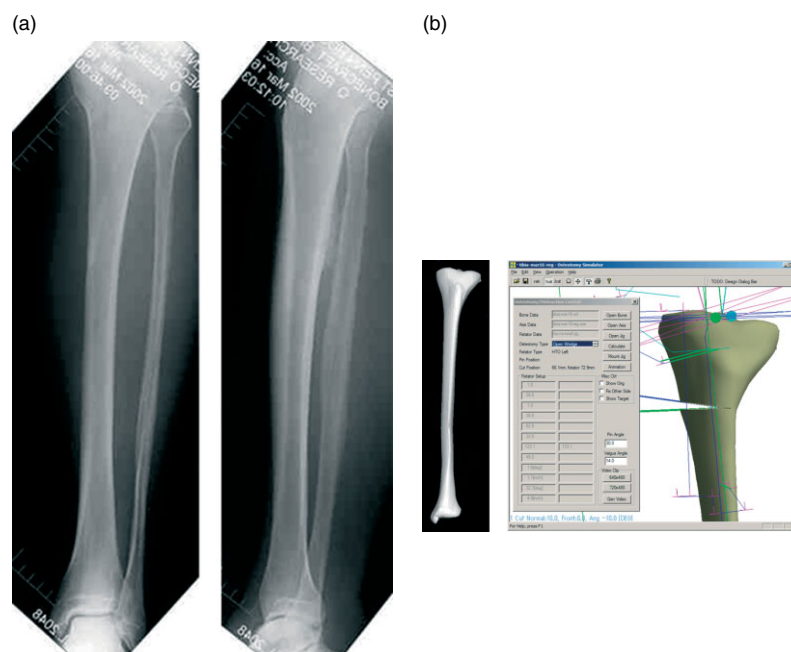


Figure 18. Cadaver study: (a) AP and LAT X-rays; (b) Reconstructed bone geometry and surgical planner

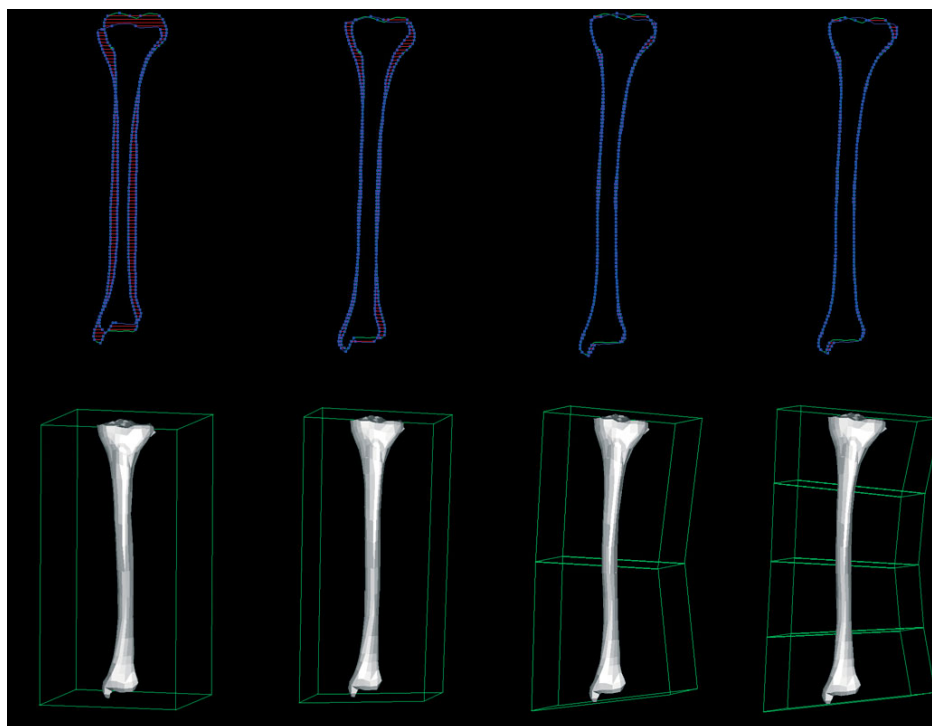


Figure 19. Hierarchical free-form deformation process of cadaver case

in Figure 14. The surgical planner generates the results which match the orthopaedic surgeon's conventional 2D surgical plan, as shown in Figure 17. Figures 15 and 16 show how the error between the silhouette boundaries of X-ray images and template bone shape is minimized through the optimization process. Note that the top portion of the tibia is more severely deformed; therefore, the finer deformation blocks are used in this region. Figure 16 shows how the optimization process converges. Moreover, the reconstructed 3D model of the tibia visually aids the orthopaedic surgeon before and during the mock surgery of this high tibial osteotomy study.

### Case study: cadaver

The purpose of this case study was to test whether the proposed reconstruction method can create a bone

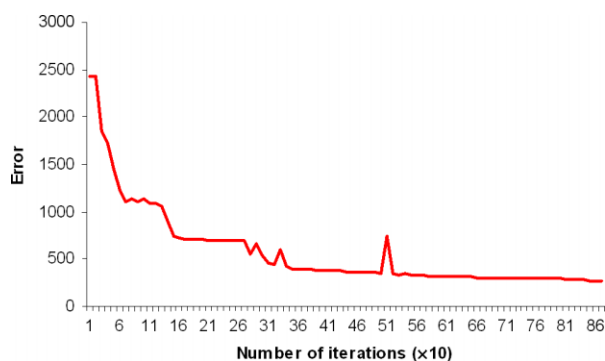


Figure 20. Minimized error between silhouette boundaries of X-ray images and template bone shape in cadaver case study

geometry with a sufficiently accurate valgus angle for the cadaver tibia. The AP and LAT X-ray images of a cadaver's right tibia, and the reconstructed 3D model, are shown in Figure 18. Based on these AP and LAT X-ray images of the cadaver, the 3D tibia shape is generated by using the proposed reconstruction method. The virtual osteotomy planner software, as shown in Figure 18, computes the necessary location for cutting, and the osteotomy angle for the changing valgus angle, from  $4^\circ$  to  $14^\circ$ , since the cadaver tibia was not deformed. The surgery was executed based on the virtual planner results with prototype surgical tool, as shown in Figure 21. The final fluoroscopic image, shown in Figure 21, demonstrates that the reconstructed 3D bone shape is sufficiently accurate for a computer-assisted orthopaedic surgery system. Furthermore, Figures 19 and 20 show how the error between the silhouette boundaries of X-ray images, and the template bone shape, is minimized through the optimization process.

### Conclusions and future work

We have presented a cost- and time-efficient computational method that takes as input X-ray images of a deformed bone and generates a 3D bone shape. The method starts with a template bone shape and deforms it until the silhouette boundaries of the template bone matches the silhouette boundaries shown in the X-ray images. By using a novel combination of hierarchical free-form deformation and numerical optimization of the deformation parameters by sequential quadratic programming, the proposed method can find a complete

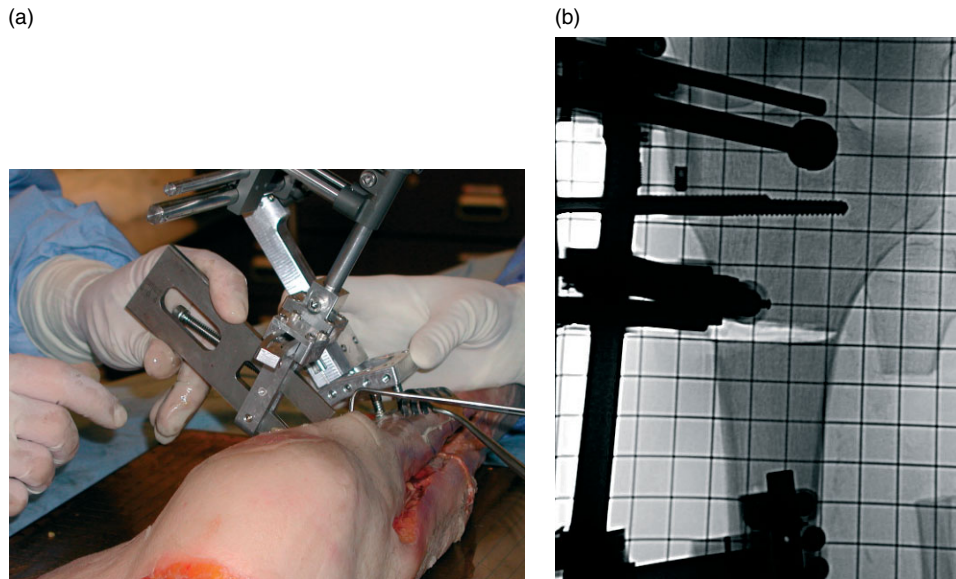


Figure 21. Execution in cadaver study: (a) execution; (b) fluoroscopic image

3D geometry. All the small features and surface texture included in the template bone data are preserved during the deformation process, making the output 3D bone look realistic.

Our X-ray image-based shape reconstruction is more computationally efficient, as well as more cost-effective and portable, compared to standard 3D sensor-based methods. Although the final 3D shape of our method can be less accurate than by using CT because of our minimum input of X-ray images, the method creates a 3D shape sufficiently accurate for most applications in training or computer-aided planning of orthopaedic surgeries, including bone distraction and open/closed wedge osteotomy.

Experimental results show that if the angle between two X-ray images is known, final reconstructed model accuracy will be improved. It can also be assumed that AP and LAT X-ray images are orthogonal to each other if the angle is between  $80^\circ$  and  $100^\circ$ . Rotational deformity of a bone smaller than  $10^\circ$  is neglected in the current reconstruction algorithm. These observations are based on the volumetric error computation method presented in (6). Furthermore, a reconstructed 3D bone model is sufficiently accurate for manufacturing a rapid prototype model, such that it can be used for training and planning of most tibial and femoral osteotomies.

## Acknowledgements

The authors would like to thank Mr Tomotake Furuhashi, Research Associate at the Computer Integrated Engineering Laboratory, for his continuous support and technical assistance; and Dr Soji Yamakawa, Research Associate at the Computer

Integrated Engineering Laboratory, for his collaborative efforts and many useful suggestions from his knowledge of computational geometry, as well as tips for implementing the algorithms.

## References

1. Lorensen WE, Cline HE. Marching cubes: a high resolution 3D surface construction algorithm. *Comput Graphics* 1987; **21**: 163–169.
2. Markowsky G, Wesley MA. Fleshing out wire frames. *IBM J Res Dev* 1980; **24**: 582–597.
3. Wesley MA, Markowsky G. Fleshing out projections. *IBM J Res Dev* 1981; **25**: 934–954.
4. Lawrence C, Zhou JL, Tits AL. *User's Guide for CFSQP Version 2.3: A C Code for Solving (Large Scale) Constrained Nonlinear (Minimax) Optimization Problems, Generating Iterates Satisfying All Inequality Constraints*. Electrical Engineering Department and Institute for Systems Research, University of Maryland: College Park, MD, 1994.
5. Stytz MR, Frieder G, Frieder O. Three-dimensional medical imaging: algorithms and computer systems. *ACM Comput Surv* 1991; **23**: 421–499.
6. Günay M. *Three-dimensional Bone Geometry Reconstruction from X-ray Images Using Hierarchical Free-form Deformation and Non-linear Optimization in Mechanical Engineering Department*. Carnegie Mellon University: Pittsburgh, PA, 2003.
7. Masuda H, Numao M. *A Cell-based Approach for Generating Solid Objects from Orthographic Projections*. IBM Research, IBM Tokyo Research Laboratory: Kanagawa, Japan, 1995.
8. Oh BS, Kim C-H. Systematic reconstruction of 3D curvilinear objects from two-view drawings. *Comput Graphics* 1999; **23**: 343–352.
9. Shin B-S, Shin YG. Fast 3D solid model reconstruction from orthographic views. *Comput Aided Design* 1998; **30**: 63–76.
10. Yan Q-W, Chen CLP, Tang Z. Efficient algorithm for the reconstruction of 3D objects from orthographic projections. *Comput Aided Design* 1994; **26**: 699–717.
11. Sederberg TW, Parry SR. Free-form deformation of solid geometric models. Presented at SIGGRAPH'86 Proceedings, Dallas, Texas, 1986.